Research Article

Superconductor superfluid density from the Bardeen–Cooper–Schrieffer/Bose crossover theory

Israel Chávez[1] · Marcela Grether[2] · Manuel de Llano[3]

© The Author(s) 2022   OPEN

Abstract

The superfluid density $n_s(T)$ of a superconductor is calculated based on the generalized Bose–Einstein condensation (GBEC) theory that addresses a fully-interacting *ternary* boson-fermion gas mixture of free electrons as fermions, plus two-electron Cooper pairs (2eCPs) and also, *explicitly*, two-hole Cooper pairs (2hCPs), both as bosons. Here we consider two special cases (i) 100%–0% (i.e., with no condensed 2hCPs) and (ii) 0%–100% (i.e., with no condensed 2eCPs). Subsumed in GBEC are the Bardeen–Cooper–Schrieffer (BCS) and Bose–Einstein condensation (BEC) theories along with the BCS-BEC crossover theory extended with 2hCPs. We find that in the weak-coupling regime $n_s(0)$ agrees with data from the Uemura et al. (2004) graph for several elemental SCs by taking in 3D with a quadratic energy-dispersion relation while in 2D with a linear relation are much too far below the data. In the strong-coupling regime the linear behavior of critical temperature T_c vs $n_s(0)$ obtained here is just as Božović et al. (2016) found. However, in 2D with a linear relation accounting for 0%–100%, $n_s(T)/n_s(0)$ compares well with some high-T_c-cuprate SC data between the two coupling regimes.

Article Highlights Superfluid density of a superconductor (SC) is calculated with the BCS-Bose crossover extended with two-hole of Cooper pairs. In the weak-coupling extreme in 3D we found good agreement with conventional SCs with quadratic dispersion relation. For high-T_c SCs (cuprates) in the intermediate coupling in 2D with a linear relation; results compare well with the data.

1 Introduction

Superfluidity in liquid ^{4}He was reported in 1938 by Kapitza [1] and independently by Allen and Misener [2] who for the first time found that the viscosity of ^{4}He drops below $T_\lambda = 2.17$ K. Almost 20 years before the Bardeen–Cooper–Schrieffer (BCS) [3] theory, Kapitza also found that this phenomenon is analogous to that of a superconductor (SC). In turn, London [4] proposed that ^{4}He is in a phase II, i.e., below T_λ, and has a Bose–Einstein condensation (BEC) behavior. The calculated BEC critical temperature of He II is $T_{BEC} = 3.1$K and so is thus slightly higher than T_λ. Landau [5–7] introduced the concept of two fluids for ^{4}He but with no connection with a BEC. Bogoliubov [8] had already shown that in a degenerate Bose gas with weak interactions there is really a BEC. Also, the existence of superfluidity turns out to be linked with BEC [9] —and indeed with Bose statistics.

✉ Israel Chávez, israelito@ciencias.unam.mx | ^{1}Instituto de Física, Universidad Nacional Autónoma de México, Apdo. Postal 20-364, Mexico City 01000, Mexico. ^{2}Facultad de Ciencias, Universidad Nacional Autónoma de México, Mexico City 04510, Mexico. ^{3}Instituto de Investigaciones en Materiales, Universidad Nacional Autónoma de México, Mexico City 04510, Mexico.

In the early 1970s Leggett [10, 11], based on experiments by Osheroff et al. [12], noted that ^{3}He atoms could in fact form BCS-like pairs. He concluded that the liquid ^{3}He phase must show [13] all phenomena associated with a BCS-like phase; he later derived [14] *two* basic crossover equations at $T = 0$ for *any* many-fermion system. In 1964 Schrieffer [15] was apparently the first to state that one must solve *two* equations, a gap-like and a number equation. This was perhaps the first BCS-Bose crossover theory. It was further developed by Keldysh [16] (1965), Popov [17] (1966), Labbé et al. [18] (1967), Eagles [19] (1969), Miyake [20] (1983), Nozières [21] (1985), Ranninger et al. [22] (1988), Randeria et al. [23, 24] (1989), Van der Marel [25] (1990), Bar-Yam [26, 27] (1991), Drechsler and Zwerger [28] (1992), Haussmann [29] (1993), Pistolesi and Strinati [30] (1996) among others.

The London penetration depth $\lambda_L = (m_e/\mu_0 n_s e^2)^{1/2}$ is the distance below a SC surface where an external magnetic field B vanishes like $B = B_0 \exp(-x/\lambda_L)$ where x is the depth inside the SC. Here m_e is the electron mass, e the elementary electron charge, μ_0 the magnetic susceptibility and n_s the superconducting electron-number density. The latter is linked with the "superelectrons"[31] of the Landau theory. In 1989 Uemura et al. [32] found a linear relationship between the critical temperature T_c of a SC and its superfluid number density n_s. It was concluded [33] that, in general, the magnitude of T_c depends on $n_s(T)$ rather than on the interelectronic coupling strength as long claimed to be true. Later, in 2016 Božović et al. [34] came to agree with these conclusions. The well-known Uemura graph [32, 33] relates the T_c of a SC with its superfluid number-density as $n_s^{2/3}/(m^*/m_e)$ where m^* is the effective electron mass and m_e its bare mass. Uemura et al. [32] [33] then suggested a *crossover* theory to correctly describe SCs. We refer to the crossover "BCS-Bose" [35, 36] instead of the more common "BCS-BEC" since a BEC cannot occur in either two dimensions (2D) nor in one dimension (1D) while bosons *can* form in both instances.

Here we corroborate the Kapitza concept that superfluidity is analogous with superconductivity, by calculating the SC superfluid density $n_s(T)$ for $T \leq T_c$ based on the generalized Bose–Einstein condensation (GBEC) theory [37–41] that includes as a special case the BCS-Bose crossover theory and also an *extended* version with two-hole Cooper pairs (2hCPs) [42] along with the more common two-electron Cooper pairs (2eCPs) ones.

In Sect. 2 the GBEC theory is recalled as it leads to the BCS-Bose extended crossover equations as a special case; in Sect. 3 the superfluid density $n_s(T)$ is introduced for two kinds of superfluids, one for 2eCPs and another for 2hCPs, the latter with an opposite charge carrier sign with respect to 2eCPs. Here we report calculated $n_s(T)$ results in 3D with a boson quadratic-dispersion relation and in 2D

with a linear-dispersion one. Comparisons are made with experimental data in 3D and 2D for some elemental and cuprate SCs. In Sect. 4 some discussion and our conclusions with future work are mentioned.

2 Generalized Bose–Einstein condensation theory

The GBEC theory starts from an ideal, noninteracting boson-fermion (BF) *ternary* gas mixture of free/unbound fermions (here electrons) plus 2eCPs and 2hCPs as bosons. To this one adds specific BF vertex interactions [37, 38] leading to a fully-interacting gas defined by the hamiltonian $H = H_0 + H_{int}$ where H_0 stands for the ideal ternary gas and H_{int} for the BF interactions.

The ideal ternary gas hamiltonian is

$$H_0 = \sum_{\mathbf{k}_1, s_1} \epsilon_{\mathbf{k}_1} a^\dagger_{\mathbf{k}_1, s_1} a_{\mathbf{k}_1, s_1} + \sum_{\mathbf{K}} E_+(K) b^\dagger_{\mathbf{K}} b_{\mathbf{K}} - \sum_{\mathbf{K}} E_-(K) c^\dagger_{\mathbf{K}} c_{\mathbf{K}}$$

(1)

here $\mathbf{K} \equiv \mathbf{k}_1 + \mathbf{k}_2$ is the center-of-mass momentum (c.m.m.) wavevector of two fermions, where $K \equiv |\mathbf{K}|$, and $\mathbf{k} \equiv \frac{1}{2}(\mathbf{k}_1 - \mathbf{k}_2)$ as their relative wavevector while $\epsilon_{k_1} \equiv \hbar^2 k_1^2/2m$ is the energy of a single fermion and $E_\pm(K) = E_\pm(0) + \hbar^2 K^2/4m$ the bosonic 2e/2hCPs phenomenological energies with $E_\pm(0)$ the bosonic energies for $K = 0$. Here $a^\dagger_{\mathbf{k}_1, s_1} (a_{\mathbf{k}_1, s_1})$ are the creation (annihilation) fermion operators, and $b^\dagger_{\mathbf{K}}(b_{\mathbf{K}})$ and $c^\dagger_{\mathbf{K}}(c_{\mathbf{K}})$ the boson operators for 2e/2hCPs. CPs are treated here as *actual* bosons in contrast with the BCS [3] "correlated" pairs which depend on their relative wavevector $\mathbf{k}$ *and* also on their total $\mathbf{K}$ wavevector whereas the original CPs [43] depend *only* on $\mathbf{K}$ [40, 41]. The former do not satisfy Bose commutation relations [3] but the latter are consistent with Bose statistics [40, 41]. The interaction hamiltonian H_{int} has four BF interaction vertices, one with two-fermion/one boson creation-annihilation operators representing how the unbound electrons (subindex +) or holes (subindex −) combine to form 2e/2hCPs in any d-dimensional system of size L. Thus

$$H_{int} = L^{-d/2} \sum_{\mathbf{k}, \mathbf{K}} f_+(k) \{ a^\dagger_{\mathbf{k}+\frac{1}{2}\mathbf{K}, \uparrow} a^\dagger_{-\mathbf{k}+\frac{1}{2}\mathbf{K}, \downarrow} b_{\mathbf{K}} + a_{-\mathbf{k}+\frac{1}{2}\mathbf{K}, \downarrow} a_{\mathbf{k}+\frac{1}{2}\mathbf{K}, \uparrow} b^\dagger_{\mathbf{K}} \}$$
$$+ L^{-d/2} \sum_{\mathbf{k}, \mathbf{K}} f_-(k) \{ a^\dagger_{\mathbf{k}+\frac{1}{2}\mathbf{K}, \uparrow} a^\dagger_{-\mathbf{k}+\frac{1}{2}\mathbf{K}, \downarrow} c^\dagger_{\mathbf{K}} + a_{-\mathbf{k}+\frac{1}{2}\mathbf{K}, \downarrow} a_{\mathbf{k}+\frac{1}{2}\mathbf{K}, \uparrow} c_{\mathbf{K}} \}.$$

(2)

where $f_\pm(k)$ are the BF interaction functions defined in Refs. [37, 38] for electrons/holes. Note that H_{int} is reminiscent of the Fröhlich interaction hamiltonian (or Dirac in QED [44] p. 36) involving two-fermion operators with a one-boson operator, but with two kinds of CPs instead of phonons/photons. Contrasting with Fröhlich and Dirac,

there is no conservation law for the number of unbound electrons, i.e., $[H_{int}, \sum_{\mathbf{k}_1,s_1} \epsilon_{\mathbf{k}_1} a^{\dagger}_{\mathbf{k}_1,s_1} a_{\mathbf{k}_1,s_1}] \neq 0$.

One can consider a simpler *reduced* H_{red} that may be written by neglecting nonzero K values and ignoring those bosons with $K \neq 0$ in H_{int}—but *not* also in H_0 as assumed in BCS theory. Applying the Bogoliubov recipe of replacing the zero-K creation operators $b^{\dagger}_0$ and $c^{\dagger}_0$ for the 2e/2hCP bosons by c-numbers $\sqrt{N_0}$ and $\sqrt{M_0}$ with N_0 and M_0 the numbers of 2e/2hCP $K = 0$ bosons. Then, using the Bogoliubov-Valatin transformation [45, 46] allows exactly diagonalizing [39] the reduced dynamical operator $\hat{H}_{red} - \mu\hat{N}$ with $\hat{N}$ the total-electron-number operator and μ a Lagrange multiplier. Bringing the neglected c.m.m. $K \neq 0$ terms back into the picture was recently implemented with two-time-Green-function techniques [47–50].

The thermodynamic (or Landau) potential of the grand-canonical statistical ensemble is now $\Omega(T, L^d, \mu, N_0, M_0) = -k_B T \ln\left[\text{Tr}(\exp\{-\beta(\hat{H}_{red} - \mu\hat{N})\})\right]$ where Tr means "trace," L^d is the system volume with d = 3, 2, 1 and $\beta \equiv 1/k_B T$ with k_B the Boltzmann constant and μ the electronic chemical potential. Thus Ω can now be evaluated explicitly. The Helmholtz free energy is then $F(T, L^d, \mu, N_0, M_0) \equiv \Omega(T, L^d, \mu, N_0, M_0) + \mu N$. Taking the negative partial derivative of Ω with respect to μ, and also minimizing the Helmholtz free energy wrt N_0 and M_0, gives

$$-\frac{\partial\Omega}{\partial\mu} = N, \qquad \frac{\partial F}{\partial N_0} = 0, \qquad \frac{\partial F}{\partial M_0} = 0. \tag{3}$$

The first equation is familiar from quantum-statistical mechanics and ensures net-charge conservation, i.e., gauge invariance [51], *not* guaranteed in BCS theory. The last two equations of (3) are needed to have a stable thermodynamic state.

From (3) the GBEC theory [37] gives three coupled, transcendental equations for three unknown T-dependent functions, the $\mu(T)$ and the 2eCP and 2hCP Bose–Einstein (BE) condensate (i.e., with $K = 0$) number densities $N_0(T)/L^3 \equiv n_0(T)$ and $M_0(T)/L^3 \equiv m_0(T)$ for 3D. The first equation of (3) leads to a *number equation* for the ternary-gas mixture in terms of the total electron-number density $N/L^3 \equiv n$ and is

$$n = 2\left[n_0(T) + n_{B+}(T) - m_0(T) - m_{B+}(T)\right] + n_f(T) \tag{4}$$

where $n_{B+}(T)$ and $m_{B+}(T)$ refer to the number densities of excited 2eCP and 2hCP bosons with $K > 0$. The free/unbound electron-number density $n_f(T)$ turns out to be

$$n_f(T) \equiv \int_0^{\infty} d\epsilon N(\epsilon)\left[1 - \frac{\epsilon - \mu}{E(\epsilon)} \tanh\{\tfrac{1}{2}\beta E(\epsilon)\}\right]$$
$$\xrightarrow[T \to 0]{} (2mE_f)^{3/2}/3\pi^2\hbar^3 \equiv n_f. \tag{5}$$

Here, E_f is viewed as a "pseudo-Fermi" energy as it refers *only* to free electrons at $T = 0$ and $E(\epsilon) \equiv \sqrt{(\epsilon - \mu)^2 + \Delta^2(T)}$ is the gapped Bogoliubov fermion-dispersion relation containing the electronic energy gap

$$\Delta(T) \equiv f_+(\epsilon)\sqrt{n_0(T)} + f_-(\epsilon)\sqrt{m_0(T)} \tag{6}$$

where $f_{\pm}(\epsilon)$ are BF vertex-interaction constants. For condensed 2eCPs

$$f_+(\epsilon) = \begin{cases} f & \text{if } E_f < \epsilon < E_f + \delta\epsilon \\ 0 & \text{otherwise} \end{cases} \tag{7}$$

and for condensed 2hCPs

$$f_-(\epsilon) = \begin{cases} f & \text{if } E_f - \delta\epsilon < \epsilon < E_f \\ 0 & \text{otherwise} \end{cases} \tag{8}$$

as originally defined in Refs. [37, 38]. Here f was taken as $f \equiv f_+ = f_-$. Here E_f and $\delta\epsilon$ are *phenomenological* energies associated with the free/unbound electrons in the BF gas mixture. E_f is related with the number density of the unbound fermions of the system $n_f(T = 0) \equiv n_f$ just as in (5). This number of unbound fermions is necessary in the calculation of the energy gap as well as in the chemical potential to obtain the superfluid density. While $\delta\epsilon$ is the energy range where the BF interactions occur and can be identified with the Debye energy of the lattice. Note that E_f coincides *exactly* with the Fermi energy E_F of an ideal fermion gas when $n_0(T) = m_0(T)$ and $n_{B+}(T) = m_{B+}(T)$, i.e., for a 50%–50% gas mixture of 2eCPs/2hCPs. For unbound electrons in 3D the density of states (DOS) is $N(\epsilon) = \left(m^{3/2}/2^{1/2}\pi^2\hbar^3\right)\epsilon^{1/2}$ and for 2D it is the constant $N(\epsilon) = m/2\pi\hbar^2$.

References [52, 53] introduce a *generalized* energy dispersion relation for the bosonic CPs. In the weak-coupling limit the dispersion relation can be expanded for small K in a series around K. In 2D one has $\varepsilon_K \xrightarrow[K\to 0]{} \varepsilon_0 + \frac{2}{\pi}\hbar v_F K + O(K^2)$ where v_F is the Fermi velocity. If $\delta\epsilon \ll E_F$ is the energy range over which the BF interaction acts in 3D and gives $\varepsilon_K \xrightarrow[K\to 0]{} \varepsilon_0 + \frac{1}{2}\hbar v_F K + O(K^2)$.

For an ideal Bose gas (IBG) consisting of pairs of fermions T_c is nonzero if $d > s$ [54] where d is the gas dimensionality and s the exponent of the bosonic CP dispersion-relation energy. As in Ref. [54] in 3D one has $s = 2$ and in 2D $s = 1$. With this one recovers the results of an IBG of two bound electrons as CPs if *all* electrons are assumed paired [55], i.e., with no unbound fermions left in the gas.

The excited (or noncondensed) boson number densities then become

$$n_{B+}(T) \equiv \int_{0+}^{\infty} d\varepsilon M(\varepsilon)\left[\exp\beta[\mathcal{E}_+(\varepsilon)] - 1\right]^{-1} \tag{9}$$

$$m_{B+}(T) \equiv \int_{0+}^{\infty} d\varepsilon M(\varepsilon)\big[\exp \beta[\mathcal{E}_-(\varepsilon)] - 1\big]^{-1} \qquad (10)$$

where $M(\varepsilon)$ is the bosonic DOS and $\mathcal{E}_\pm(\varepsilon) = \pm 2E_f + \delta\varepsilon \mp 2\mu + \varepsilon$ the energy of excited 2e/2hCPs. For the 3D IBG with $s = 2$ one has

$$M(\varepsilon) = (2m^{3/2}/\pi^2\hbar^3)\sqrt{\varepsilon} \qquad (11)$$

and in 2D with $s = 1$[54]

$$M(\varepsilon) = 2\pi\big(\delta\varepsilon/2\tilde{G}_{2D}\hbar v_F\big)^2 \varepsilon + \mathcal{O}(\varepsilon^2). \qquad (12)$$

We introduce $\tilde{G}$ a BF dimensionless strength interaction in 2D which in turn is related with the BF vertex-interaction constants f as

$$\tilde{G}_{2D} \equiv f^2 m_e/8\pi\hbar^2 E_F \qquad \tilde{G}_{3D} \equiv f^2 m_e^{3/2}/2^{5/2}\pi^2\hbar^3 E_F^{1/2} \qquad (13)$$

where the second equation is in 3D, last defined in Refs. [37, 38]. The Bose distributions in (9) and (10) are clear indications of the bosonic nature of both kinds of CPs. In 3D the BF strength interaction can be related with the BCS dimensionless coupling parameter λ_{BCS} as $G_{3D} = \lambda_{BCS}\delta\varepsilon_{3D}/2$ and in 2D as $G_{2D} = \lambda_{BCS}\delta\varepsilon_{2D}/4$.

The second equation in (3) gives a *gap-like equation* for 2eCPs

$$2\sqrt{n_0(T)}[2E_f + \delta\varepsilon - 2\mu(T)] = \int_0^\infty d\varepsilon N(\varepsilon)\frac{\Delta(\varepsilon)f_+(\varepsilon)}{E(\varepsilon)}\tanh\left[\tfrac{1}{2}\beta E(\varepsilon)\right] \qquad (14)$$

and the third equation in (3) the same, but for 2hCPs

$$2\sqrt{m_0(T)}[2\mu(T) - 2E_f + \delta\varepsilon] = \int_0^\infty d\varepsilon N(\varepsilon)\frac{\Delta(\varepsilon)f_-(\varepsilon)}{E(\varepsilon)}\tanh\left[\tfrac{1}{2}\beta E(\varepsilon)\right]. \qquad (15)$$

We then have three special cases, namely

  (i)　50%–50% proportions between 2eCPs and 2hCPs, i.e., $n_0(T) = m_0(T)$ and $n_{B+}(T) = m_{B+}(T)$ solving simultaneously (14) plus (15) with (4),

  (ii)　100%–0%, i.e., $m_0(T) = 0$ solving simultaneously (14) with (4) and

  (iii)　0%–100%, i.e., $n_0(T) = 0$ solving simultaneously (15) with (4).

The set of equations (14), (15) and (4) are called as the *extended* BCS-Bose crossover equations with *explicit* inclusion of 2hCPs [42] and contains a dimensionless coupling parameter n/n_f with n the total number density and n_f that for unbound electrons at zero absolute temperature. We found two distinct coupling regimes, namely i) *weak* coupling for $n/n_f = 1$ when *all* electrons are unbound, albeit like "correlated" pairs as in BCS theory, with $\mu(T = 0) = E_F$; ii) *strong* coupling when $n/n_f \to \infty$ as when, e.g., $n_f \to 0$,

meaning that *all* electrons are paired into CPs implying an IBG consisting of 2eCPs when $\mu(T)/E_F \to 0$. Here $n/n_f = 10^6$ is virtually the strong-coupling extreme; and iii) an *intermediate* regime between weak- and strong-coupling when $1 < n/n_f < \infty$. Varying this parameter from $n/n_f = 1$ one can describe elemental superconductors. Changing n/n_f slightly from unity one can address SCs like Pb and Hg which are known as "bad actors" [56] in BCS theory.

In the extended BCS-Bose crossover one calculates [57] the ratio $T_c/T_F \equiv k_B T_c/E_F$ for several elemental superconductors including the BCS theory "bad actors" Hg and Pb. This was reported in Ref. [57] for the energy gap in the 50%–50% case and found to agree to with the data, whereas the 100%–0% case [i.e., when $m_0(T) = 0$] lies too far below data trends and likewise for the 50%–50% case. This already suggests that condensed 2hCPs might be necessary to correctly describe any SC. Recall that from Ref. [37] 2hCPs are indispensable in a BCS condensate which *must* be a 50%–50% mixture to give the BCS gap equation exactly for all couplings and all Ts as well as the full condensation energy for $T = 0$.

3　Superconductor superfluid density

In the extended-crossover theory the T-dependent superfluid number density $n_s(T)$ involves only those CPs either in the ground/excited state for $T \le T_c$. One can then define $n_s(T)$ as

$$\begin{aligned}n_s(T) &\equiv n - n_f(T) \\ &= 2\big[n_0(T) + n_{B+}(T) - m_0(T) - m_{B+}(T)\big]\end{aligned} \qquad (16)$$

where n is the total number density (4) and $n_f(T)$ that of unbound electrons (5). Here, the superfluid density (SFD) (16) resembles the SFD of the Landau two-fluid model [5–7] where the total *mass* density is $\rho = \rho_s + \rho_n$ with ρ_s the superfluid mass density and ρ_n SFD with Bose statistics since in (16) there are only CPs as bosons.

There are two special cases: i) $m_0(T) = 0$, i.e., there are no condensed 2hCPs, so one has the 100%–0% case and the SFD is

$$n_{s,2e}(T) = 2\big[n_0(T) + n_{B+}(T) - m_{B+}(T)\big] \qquad (17)$$

and ii) $n_0(T) = 0$, i.e., there are no condensed 2eCPs, one has in the 0%–100% case

$$n_{s,2h}(T) = 2\big[-m_0(T) + n_{B+}(T) - m_{B+}(T)\big]. \qquad (18)$$

The more general case (16) includes both kind of CPs, while 100%–0% and 0%–100% cases one have ignored one kind of condensed CPs. To find the superfluid density in this extended crossover one must solve the set equations (14), (15) and (4) to have the energy gap as well as the

chemical potential, both dependent of temperature. These values must be substituted in (16), (17) and (18).

Figure 1a shows a phase diagram of the dimensionless superfluid density $n_s(0)/n$ vs. the dimensionless number density n/n_f for the 100%–0% case using (17) and for the 0%–100% case using (18) in 3D with a quadratic energy-dispersion relation as well as in 2D with linear relation. If one takes the 50%–50% proportions in (16) one sees that $n_s(T) = 0$ implying that both kinds of CPs cannot contribute to SFD in any coupling regime while the 100%–0% and 0%–100% cases can do. Taking the weak-coupling extreme, i.e., when $n/n_f = 1$ the 100%–0% and 0%–100% cases cannot contribute to SFD, one must take $n/n_f \neq 1$. Taking $n/n_f \simeq 10^3$ one sees that the 100%–0% case in 3D as well as in 2D all electrons are paired, i.e., one has an ideal Bose gas composed of 2eCPs. The 0%–100% case with $n/n_f = 0.5$ all holes paired into 2hCPs. Thus n/n_f becomes our interest here since taking $n/n_f = 1$ all particles are unbound, implying that $n/n_f > 1$ electrons paired into CPs and taking $n/n_f < 1$, holes paired into 2hCP. However, the proper interpretation of $n < n_f$ is that the number density of unbound fermions are greater than the total number density, but this leads to a disagreement, instead one might suppose that occurs an insertion of particles to the system, in this case a finite number of 2hCPs, this suggests that the system can be doped with holes.

In Fig. 1b the critical temperature T_c is plotted for the 100%–0% and 0%–100% cases vs $n_s(0)/n$ in both 2D and 3D. Shows the 100%–0% case with a special case where $m_{B+}(T) = 0$, i.e., the excited 2hCPs bosons has been ignored, with a *linear* energy-dispersion relation in 2D and with a *quadratic* relation in 3D. The 0%–100% case enhances the critical temperature at relatively low SFD. Note that $n_s(0)/n$ has a linear behavior in the strong-coupling regime as reported in Ref. [34, Fig. 2d] for T_c vs ρ_{s0} SFD of data where $\rho_{s0} \equiv \rho_s(T \rightarrow 0)$ from this reference. The mere presence of excited 2hCPs enhances the value of T_c [40, 41]. This is exactly analogous to the increase, at higher and higher temperatures, of antibosons (here 2hCPs) in the *relativistic* IBG [58].

As mentioned above, the weak-coupling (BCS) regime is when one considers the 50%–50% proportions. Thus in (4) at $T = 0$ one has $n/n_f = 1$ meaning that the rest of fermions remain unbound. This limit resembles a fermion system interacting via an attractive potential [21] when $N = N_f$, i.e., sufficiently high fermion densities [59]. The BEC regime is achieved when all fermions are bound as pairs, i.e., the fermion density decrease while boson density increase, namely, the number density ratio changes as $1 \leq n/n_f < \infty$. These properties are described in the phase diagram T_c/T_F vs n/n_f in but is here extended with the dimensionless SFD $n_s(0)/n$, which is illustrated in Fig. 2 in 3D. The phase diagram of Fig. 2 describes
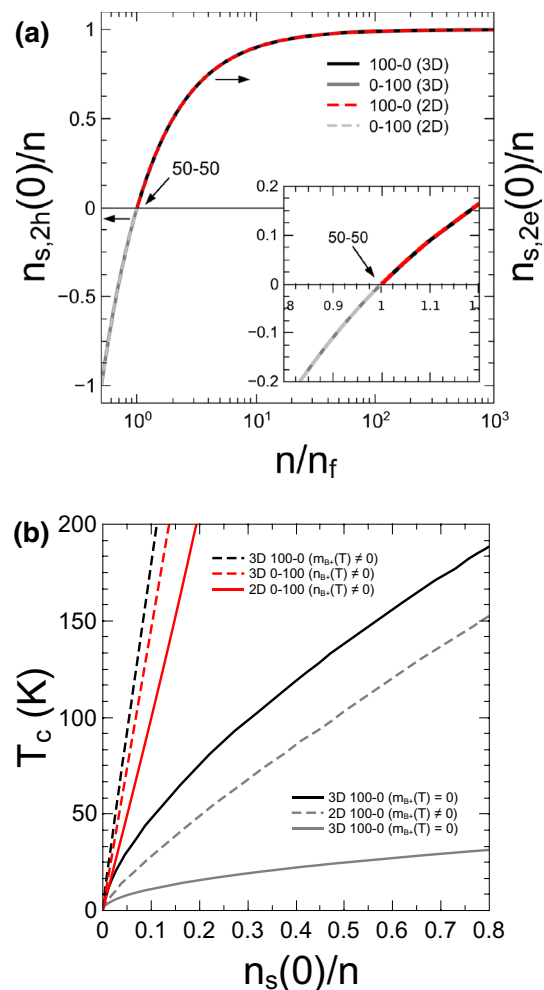

Fig. 1 (Color online) **a** Dimensionless superfluid density $n_s(0)/n$ vs. n/n_f for 100%–0% (black full) curve, 0%–100% (gray-dashed) curve using (17) and (18), respectively, for 3D and 100%–0% (red dashed) curve, 0%–100% (gray dashed) curve using the same equations for 2D. When $n/n_f \simeq 10^3$ one have $n_{s,2e}(0)/n \simeq 1$ and when $n/n_f \simeq 0.5$ one has $n_{s,2h}(0)/n \simeq -1$. One has the negative sign in the superfluid density of 0%–100% case, this is consistent with 2hCPs charge carriers sign in (4). Inset shows the behavior of superluid density near $n/n_f = 1$ (weak coupling) extreme. Also there is a sign symmetry with respect this point between 100%–0% and 0%–100% cases. **b** Critical temperature T_c vs $n_s(0)/n$ from the extended crossover theory for the 100%–0% and 0%–100% cases in 3D and 2D, $m_{B+}(T) = 0$ indicate that excited 2hCPs have been ignored and $n_{B+}(T) = 0$ that excited 2eCPs have also been ignored. Note that the mere presence of 2hCPs enhance critical temperatures. One can see a linear behavior still holds at relatively high superfluid densities, this linear behavior holds in the strong-coupling regime as Božović et al. [34] found in their Fig. 2d. Here $\tilde{G} = 10^{-4}$ and $\delta\tilde{\epsilon} = 10^{-3}$ were used; "tilde" meaning made dimensionless with the Fermi energy E_F

the behavior of the dimensionless SFD at $T = 0$ when the dimensionless number density varies as function of T_c/T_F. For 100%–0% case in the strong-coupling regime when $n/n_f > 10^2$ almost all fermions as pairs are in the superfluid state, while for 0%–100% case this occur when

$n/n_f \rightarrow 1/2$, but the 50%–50% case the dimensionless SFD is zero as shown before. Also, note that T_c/T_F increases linearly as the dimensionless SFD increases in the strong-coupling regime as Uemura et al. [32, 33] and independently Božović et al. [34] found. The region of arbitrary proportions between 2eCPs and 2hCPs may lie between the white-orange (100-0) surface and light-blue (0-100) surface.

Table 1 lists superfluid density $n_s(T = 0)$ experimental values and also calculated with the extended-crossover set of equations (17) and (18) for 100%–0% and 0%–100%
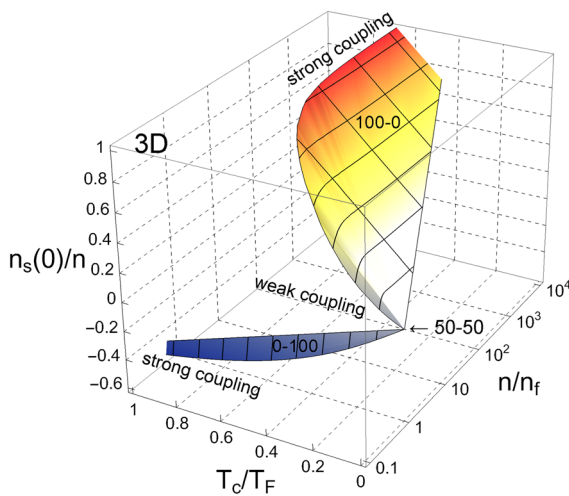
Fig. 2 Phase diagram n/n_f vs T_c/T_F vs $n_s(0)/n$ for the 100%–0% (white-red surface) and 0%–100% (light-blue surface) cases in 3D of the extended BCS-Bose crossover. The weak-coupling regime is when $n/n_f = 1$ there is a high unbound fermion density, while the strong-coupling regime occurs when $n/n_f > 10^2$ for the 100%–0% case and $n/n_f \rightarrow 1/2$ for the 0%–100% case with high boson density. Note that T_c/T_F increases linearly as the dimensionless SFD increases just as Uemura et al. [32, 33] and, independently, Božović et al. [34] found

cases, respectively, taking specifically $n/n_f = 1.00001$ for 100%–0%, meaning that the number density of unbound electrons is 0.001% smaller than the total number density. For 0%–100% $n/n_f = 0.99999$ was used meaning that the number density of unbound holes is 0.001% greater than of that total number density, i.e., it has been inserted as finite number of 2hCP. These values of the dimensionless number density are near the weak coupling extreme (BCS theory) for elemental superconductors. They are compared with data from Ref. [33] in 2D. In 3D as $n_{s,3D}^{2/3}(T = 0)$ with a quadratic energy-dispersion relation and in 2D simply as $n_{s,2D}(T = 0)$ and with a linear relation. Note that the 3D results agree with data trends, while in 2D results have some orders of magnitude below even from the 3D case.

Also shown is the penetration depth $\lambda^2 \propto m^\star/n_s$ results in 3D. Results of the 100%–0% case for Zn are near the data while the 0%–100% case is so for Al, Sn and Nb, while the 2D cases are not reported since the SFD are too far below of data. But it needs the Pippard coherence length of the 2e/2hCPs to have a complete picture of the penetration depth. Here we used the effective electron mass in 3D for the calculations in 3D and 2D. Also listed are the BF parameters as $\delta\tilde{\epsilon}$ and $\tilde{G}$ for each SC. Future work will be to use the effective mass tensor.

For an ultracold bosonic atomic gas one must solve the 100%–0% case, i.e., with $m_0(T) = m_{B+}(T) = 0$. This is analogous to an IBG gas when $n/n_f \rightarrow \infty$, e.g., when $n_f = 0$. Here 2hCPs contributions can be neglected as their numbers are likely negligible at the very low densities associated with a shallow Fermi sea is expected [60] to accommodate only a tiny number of holes. Ignoring them, one recovers the limits of T_c/T_F when $n/n_f \rightarrow \infty$. For the extended crossover in 3D giving $T_c/T_F \rightarrow 0.204$ and in 2D $T_c/T_F \rightarrow 0.034$ so that $n_s(0)/n \rightarrow 1$ as expected [55]. Results in Table 1 suggest again the connection between superfluid density and Bose statistics. The $_2^4$He

Table 1 Values of $n_{s3D}(T = 0)^{2/3}/(m^*/m_e)$ with a *quadratic* energy dispersion relation and $n_{s2D}(T = 0)/(m^*/m_e)$ with a *linear* relation, calculated with the extended BCS-Bose crossover theory using (17) for the 100%–0% case with $n/n_f = 1.00001$ and (18) for the 0%–100% case with $n/n_f = 0.99999$ in 2D and 3D

| | T_c/T_F ($\times10^{-5}$) | | $n_{s3D}^{2/3}(0)/m^*$ (cm^{-2}) | | | $n_{s2D}(0)/m^*$ (cm^{-2}) | | $\lambda_{L,3D}(0)$ (nm) | | | BF parameters | |
	Exptl	Extended	Exptl	100%–0%	0%–100%	100%–0%	0%–100%	Exptl	100%–0%	0%–100%	$\delta\tilde{\epsilon} \times 10^3$	$\tilde{G} \times 10^4$
Zn	0.80	0.79	2.31×10^{15}	3.32×10^{15}	6.10×10^{14}	1.71×10^{13}	1.12×10^{13}	18.4	17.3	40	2.1	1.8
Al	0.87	0.86	4.90×10^{15}	1.05×10^{15}	1.88×10^{15}	7.74×10^{11}	7.74×10^{12}	16.9	30.8	30.8	3.0	2.5
Sn	3.15	3.13	3.00×10^{15}	8.27×10^{15}	2.61×10^{15}	9.63×10^{13}	7.18×10^{12}	20.9	10.9	26.2	1.6	2.0
Nb	14.96	14.90	4.00×10^{14}	1.61×10^{15}	1.15×10^{14}	3.91×10^{13}	4.10×10^{11}	173	24.8	321.8	4.4	6.2
$_2^4$He	0.19	0.20	3.25×10^{11}	2.05×10^{11}	–	1.93×10^{11}	–	–	–	–	10	10

These are compared with empirical data of Uemura et al. [33] for four typical elemental SCs near the weak-coupling regime. Note that 3D cases reproduce the data trends while the 2D cases do not. For the ultracold atomic gas of $_2^4$He atoms $n/n_f \simeq 10^6$ (strong-coupling regime) was used. Values for m^*/m_e for each SC are from Ref. [61] and for $_2^4$He from [62]. Also listed is the penetration depth $\lambda_L^2 \propto m^*/n_s$ in 3D. The last two columns list the BF parameters for each superconductor

case is worth mentioning too because all fermions are supposed to be paired for extremely strong coupling, viz., $n/n_f \to \infty$, leaving essentially an IBG so that the calculated superfluid density agrees with the data. This suggests that this BF mixture with the 100%–0% case *can* describe successfully ultracold fermionic atomic clouds.

Figure 3a shows calculated 2D superfluid density $n_s(T)/n_s(0)$ vs T/T_c curves with a linear dispersion relation using (17) and (18) compared with HTSC data [63–65]. Also plotted is the 100%–0% case near weak coupling with $n/n_f = 1.00005$ and the intermediate coupling with $n/n_f = 100$. The former approximates better the data trends but the latter is too far below the data. Also plotted is the 0%–100% case near weak coupling with $n/n_f = 0.99999$ and $n/n_f = 0.997$. The former appears to mean that 0.001% of unbound holes have been inserted while the latter with 0.3%. If one varies $n/n_1 \neq 1$ with 2hCPs one can adjust to data trends. This suggests that this HTSC *cannot* be correctly described by a 50%–50% mix of 2eCPs/2hCPs in the weak-coupling regime.

Figure 3b shows the 3D superfluid density $n_s(T)/n_s(0)$ vs T/T_c with a quadratic relation compared with the same HTSCs data [63–65] previously shown. Shows the weak-coupling regime solving (17) and (18), these two cases are so far from data but they are near of the SFD curve of BCS theory, this suggesting that this HTSC *cannot* be explained by weak-coupling BCS theory, as long suspected. But if one changes $n/n_f \neq 1$ both curves come together with the general behavior but not adjust to data. This suggests that the 3D case cannot describe at all the HTSC data.

In 3D, the 100–0% as well as the 0%–100% cases near weak-coupling regime, i.e., with $n/n_f = 1$ is too far from the data and also from the BCS curve. Thus, these cuprates cannot be correctly described with weak-coupling assumptions. However, for these SC cuprates occurs in cuasi-2D as in $La_{2-x}Sr_xCuO_4$ with $x = 0.21$[64]. In 2D, the 100%–0% as well as 0%–100% curves with $n/n_f \simeq 1$ does describe the general behavior, although the 0%–100% case changing as $0.997 \leq n/n_f \leq 0.99999$ can adjust the data, suggesting that charge carriers are 2hCPs. This suggests that this SC might lie between a BF mixture with $n/n_f = 1$ and $n/n_f = 10^2$, i.e., in the intermediate-coupling regime.

4 Discussion

From Kaptiza's arguments on the superfluid density and from definitions of (17) and (18), the 2eCPs and the 2hCPs contribute to the superfluid density. The extended crossover leads to the important concept of "three components" since one here deals with a ternary gas. Taking
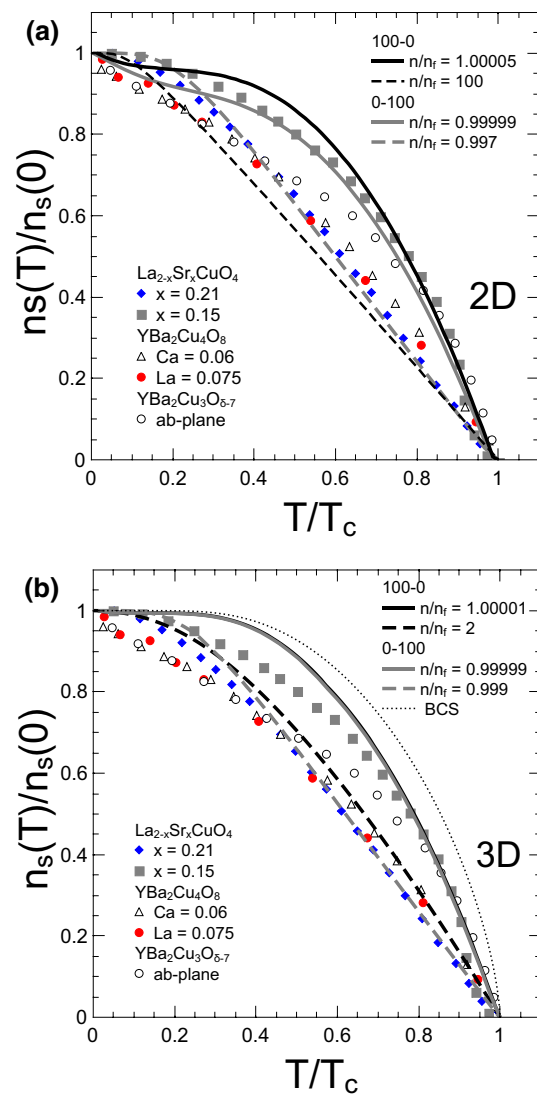
Fig. 3 (Color online) **a** 2D superfluid density $n_s(T)/n_s(0)$ vs T/T_c from the extended crossover for 100%–0% case using (17) black-full curve with $n/n_f = 1.00005$ near weak coupling and the black-dashed curve with $n/n_f = 100$ strong-coupling regime. For 0%–100% case using (18) gray-full curve with $n/n_f = 0.99999$ and gray-dashed curve with $n/n_f = 0.997$ each compared with HTSC data of $YBa_3CuO_{\delta-7}$ ab-plane [63] (open circles); $La_{2-x}Sr_xCuO_4$ [64] (gray squares) $x = 0.15$ (blue-online diamonds) $x = 0.21$; $YBa_2Cu_4O_8$ [65], Ca = 0.06 (open triangles) and La = 0.075 (red online circles). There is two important cuprate-SC results shown here between the 100%–0% and 0%–100% cases near the weak coupling regime and between the 100%–0% strong-coupling regime and 0%–100% gray-dashed case suggesting that these SCs might be correctly described by bosonic 2hCPs in 2D. **b** 3D superfluid density $n_s(T)/n_s(0)$ vs. T/T_c from the extended-crossover theory for 100%–0% case using (17) black-full curve with $n/n_f = 1.00001$ near weak coupling and the black-dashed curve with $n/n_f = 2$ intermediate coupling. For the 0%–100% case using (18) gray-full curve with $n/n_f = 0.99999$ and gray-dashed curve with $n/n_f = 0.999$ each compared with HTSC data and BCS (dotted-gray) curve is included for comparison purposes only. Finally, near weak-coupling regime the 3D case is far from data trends

the 50%–50% mixture of 2eCPs/2hCPs, i.e., $n_0(T) = m_0(T)$ and $n_{B+}(T) = m_{B+}(T)$ implying that $n_s(T) = 0$; this result drastically contrasts with the results of the energy gap or the critical temperature [42]. This result is quite different, even for the BCS-theory superfluid density it was assumed to be a symmetrical distribution between 2eCPs and 2hCPs, this symmetry remains unclear in their superfluid density. Furthermore, in the London penetration depth related with superconductor density there is no mention on what kind of charge carriers are involved, even as it's supposed to be negative charge carriers, i.e., electrons. We have considered this kind of symmetry and obtained good results [57]. Thus, in definitions given in (17) and (18) there are two kinds of specific contributions of condensed 2eCPs/2hCPs as well as excited 2e/2hCPs. The main advantage of the extended crossover theory seems to be the *explicit* inclusion of 2hCPs. This addition of 2hCPs might be interpreted as doping since the number density has been increased.

Two independent groups, Uemura et al. [32, 33] and Božović et al. [34], have found that the critical temperature T_c has a linear relationship with the superfluid density, rather than with the coupling strength as commonly held. This is illustrated in Fig. 1b showing T_c vs superfluid density of 2eCPs after using (17) for 100%–0% cases. It's worth mentioning here that the 0%–100% case enhanced T_cs with relatively low SFDs. Also, one sees that in the range of intermediate- to strong-coupling regime clearly showing that regardless of the pair-coupling strength the linear relationship between superfluid density and T_c can, in fact, be explained by an increase of the number of 2eCPs as many have long claimed, at least in 2D, and also with the explicitly inclusion of *excited* 2hCPs.

5 Conclusions

The superfluid density $n_s(T)$ was calculated with the extended-crossover theory from the GBEC theory. In the weak-coupling regime, in 3D $n_s(T = 0)$ agrees with the Uemura et al. [32] data for the elemental SCs like Zn, Al, Sn and Nb. However, the quadratic energy-dispersion relation in 3D gives a better approach to the superfluid density reported, at least for the elemental SCs since here can be addressed with a BF gas mixture in 3D. Regarding all of this, there are at least *five* thermodynamic scenarios, e.g., see Ref. [57], which show that a lack of 2hCPs decreases the energy-gap size and also that of the gap-to-T_c ratio from well-known data, leading one to conclude *unequivocally* that condensed 2hCPs are indeed *indispensable* to correctly describe SCs. However, in the strong-coupling regime

$n_s(T)$ for ultracold-bosonic-atomic clouds of, e.g., $^4_2$He, in the 100%–0% case [i.e., with $m_0(T) = m_{B+}(T) = 0$ and $n/n_f \simeq 10^6$] agrees remarkably well with the data, indicating that condensed ultracold bosonic gases behave like ordinary BE condensates. Also, the superfluid density $n_s(0)/n$ in strong coupling is seen to have a linear behavior with T_c just as Božović et al. [34] found. Hence, HTSC data can be described reasonably well with a BF mixture using the 100%–0% and the 0%–100% cases between weak- and strong-coupling in 2D by changing the number density of the unbound fermions.

Future work will focus on $n_s(T)$ using the 0%–100% case for some other HTSCs and for ultracold-fermionic-atomic clouds [66, 67] including BF gas mixtures like $^4_2$He / $^3_2$He and also with the critical magnetic field $H^2_c(T,n)/8\pi$ of the superfluid density from the extended-crossover theory. Also, the dimensionless number density that we used since a coupling parameter has been changed slightly and is not big enough to note any singular phenomena. This will be dealt with in another paper. However, it seems to us necessary to address the electronic structure in this BF theory; this might improve the results shown here. The electronic structure study will be discussed elsewhere as part of future work.

Declaration

Conflicts of interest All authors declare no conflict of interest.

References

1. Kapitza P (1938) Viscosity of liquid helium below the λ-point. Nature 141:74. https://doi.org/10.1038/141074a0
2. Allen J, Misener A (1938) Flow of liquid helium Il. Nature 141:75. https://doi.org/10.1038/141075a0
3. Bardeen J, Cooper L, Schrieffer J (1957) Theory of superconductivity. Phys Rev 108:1175. https://doi.org/10.1103/PhysRev.108.1175
4. London F (1938) The λ-phenomenon of liquid helium and the Bose-Einstein degeneracy. Nature 141:643–644. https://doi.org/10.1038/141643a0
5. Landau LD (1941) The theory of superfuidity of helium II. J Phys USSR 5:71–100 (1941)
6. Landau LD (1947) The theory of superfluidity of helium II. J Phys USSR 11:91
7. Landau LD (1949) On the theory of superfluidity. Phys Rev 75:884. https://doi.org/10.1103/PhysRev.75.884
8. Bogoliubov NN (1947) On the theory of superfluidity. J Phys USSR 11:23–32
9. Balibar S (2007) The discovery of superfluidity. J Low Temp Phys 146:441–470. https://doi.org/10.1007/s10909-006-9276-7
10. Leggett AJ (1972) Interpretation of recent results on He^3 below 3 mK: a new liquid phase? Phys Rev Lett 29:1227. https://doi.org/10.1103/PhysRevLett.29.1227
11. Leggett AJ (2004) Nobel lecture: superfluid ^3He: the early days as seen by a theorist. Rev Mod Phys 76:999. https://doi.org/10.1103/RevModPhys.76.999
12. Osheroff DD, Richardson RC, Lee DM (1972) Evidence for a new phase of solid He^3. Phys Rev Lett 28:885. https://doi.org/10.1103/PhysRevLett.28.885
13. Anderson PW, Morel P (1961) Generalized Bardeen-Cooper-Schrieffer states and the proposed low-temperature phase of liquid He^3. Phys Rev 123:1911. https://doi.org/10.1103/PhysRev.123.1911
14. Leggett AJ (1980) Cooper pairing in spin-polarized fermi systems. J Phys Colloques 41:C7-19–C7-26. https://doi.org/10.1051/jphyscol:1980704
15. Schrieffer JR (1963) Theory of superconductivity. Benjamin, New York, p 41
16. Keldysh LV, Kopaev YV (1965) Possible instability of the semimetallic state toward coulomb interaction. Sov Phys Sol St 6:2219
17. Popov VN (1966) Theory of a Bose gas produced by bound states of fermi particles. Sov Phys JETP 50:1034
18. Labbé J, Barišić F, Friedel J (1967) Strong-coupling superconductivity in V_3X type of compounds. Phys Rev Lett 19:1039. https://doi.org/10.1103/PhysRevLett.19.1039
19. Eagles DM (1969) Possible pairing without superconductivity at low carrier concentrations in bulk and thin-film superconducting semiconductors. Phys Rev 186:456. https://doi.org/10.1103/PhysRev.186.456
20. Miyake K (1983) Fermi liquid theory of dilute Submonolayer ^3He on thin ^4He II film: dimer bound state and cooper pairs. Prog Theor Phys 69:1794–1797. https://doi.org/10.1143/PTP.69.1794
21. Noziéres P, Schmitt-Rink S (1986) Bose condensation in an attractive fermion gas: From weak to strong coupling superconductivity. J Low Temp Phys 59:195–211. https://doi.org/10.1007/BF00683774
22. Ranninger J, Micnas R, Robaszkiewicz S (1988) Superconductivity of a mixture of local pairs and quasi free electrons. Ann Phys Fr 13(5):455–464. https://doi.org/10.1051/anphys:01988001305045500
23. Randeria M, Duan JM, Shieh LY (1989) Bound states, Cooper pairing, and Bose condensation in two dimensions. Phys Rev Lett 62:981. https://doi.org/10.1103/PhysRevLett.62.981
24. Randeria M, Duan JM, Shieh LY (1989) Erratum Phys Rev Lett 62:2887. https://doi.org/10.1103/PhysRevLett.62.2887
25. van der Marel D (1990) Anomalous behaviour of the chemical potential in superconductors with a low density of charge carriers. Physica C 165:3543. https://doi.org/10.1016/0921-4534(90)90429-I
26. Bar-Yam Y (1991) Two-component superconductivity. I. Introduction and phenomenology Phys Rev B 43:359- https://doi.org/10.1103/PhysRevB.43.359
27. Bar-Yam Y (1991) Two-component superconductivity. II. Copper oxide high-T_c superconductors 43:2601 https://doi.org/10.1103/PhysRevB.43.2601
28. Drechsler M, Zwerger W (1992) Crossover from BCS superconductivity to Bose condensation. Ann. der Physik 1:15–23. https://doi.org/10.1002/andp.19925040105
29. Haussmann R (1994) Properties of a Fermi liquid at the superfluid transition in the crossover region between BCS superconductivity and Bose-Einstein condensation. Phys Rev B 49:12975. https://doi.org/10.1103/PhysRevB.49.12975
30. Pistolesi F, Strinati GC (1996) Evolution from BCS superconductivity to Bose condensation: calculation of the zero-temperature phase coherence length. Phys Rev B 53:15168. https://doi.org/10.1103/PhysRevB.53.15168
31. Fujita S, Godoy S (2002) Quantum statistical theory of superconductivity. Kluwer Academic Publishers, New York, p 258
32. Uemura YJ et al (1989) Universal correlations between T_c and n_s/m^* (carrier density over effective mass) in high-T_c Cuprate superconductors. Phys Rev Lett 62:2317. https://doi.org/10.1103/PhysRevLett.62.2317
33. Uemura YJ (2004) Condensation, excitation, pairing, and superfluid density in high-T_c superconductors: the magnetic resonance mode as a roton analogue and a possible spin-mediated pairing. J Phys Cond Matter 16(40):S4515–S4540. https://doi.org/10.1088/0953-8984/16/40/007
34. Božović I, He X, Wu J et al (2016) Dependence of the critical temperature in overdoped copper oxides on superfluid density. Nature 536:309–311. https://doi.org/10.1038/nature19061
35. Quick RM, Esebbag C, de Llano M (1993) BCS theory tested in an exactly solvable fermion fluid. Phys Rev B 47:11512. https://doi.org/10.1103/PhysRevB.47.11512
36. Adhikari SK, de Llano M, Sevilla FJ, Solís MA, Valencia JJ (2007) The BCS-Bose crossover theory. Physica C 453:37–45. https://doi.org/10.1016/j.physc.2006.12.004
37. Tolmachev VV (2000) Superconducting Bose-Einstein condensates of Cooper pairs interacting with electrons. Phys Lett A 266:400–408. https://doi.org/10.1016/S0375-9601(00)00079-7
38. de Llano M, Tolmachev VV (2003) Multiple phases in a new statistical boson-fermion model of superconductivity. Phys A 317:546–564. https://doi.org/10.1016/S0378-4371(02)01348-1
39. de Llano M, Tolmachev VV (2010) A generalized Bose-Einstein condensation theory of superconductivity inspired by Bogolyubov. Ukr Phys J 55:79–84
40. Grether M, de Llano M, Tolmachev VV (2013) A generalized BEC picture of superconductors. Int J Quant Chem 112:3018–3024. https://doi.org/10.1002/qua.24193
41. Grether M, de Llano M, Tolmachev VV (2013) Generalized Bose-Einstein condensation formalism and BCS theory. J Supercond Nov Magn 26:1915–1919. https://doi.org/10.1007/s10948-012-2054-7
42. Chávez I, García LA, Grether M, de Llano M, Tolmachev VV (2018) Extended BCS-Bose crossover. J Supercond Nov Magn 31:631–637. https://doi.org/10.1007/s10948-017-4383-z

43. Cooper LN (1956) Bound electron pairs in a degenerate fermi gas. Phys Rev 104:1189–1190. https://doi.org/10.1103/PhysRev.104.1189

44. Fetter AL, Walecka JD (1971) Quantum theory of many-particle systems. McGraw-Hill, New York

45. Bogoliubov NN (1958) A new method in the theory of superconductivity. I. Sov Phys JETP 34:41-46 (1958)

46. Valatin JG (1958) Comments on the theory of superconductivity. Nuovo Cim 7:843–857. https://doi.org/10.1007/BF02745589

47. Mamedov TA, de Llano M (2010) Superconducting Pseudogap in a Boson-Fermion model. J Phys Soc Jpn 79:044706–044714. https://doi.org/10.1143/JPSJ.79.044706

48. Mamedov TA (2011) de Llano. Generalized Superconducting Gap in an Anisotropic Boson-Fermion Mixture with a Uniform Coulomb Field. 80:074718–074725. https://doi.org/10.1143/JPSJ.80.074718

49. Mamedov TA, de Llano (2013) Depairing and Bose-Einstein condensation temperatures in a boson-fermion superconductor model with Coulomb effects. Phil Mag 93:2896–2912. https://doi.org/10.1080/14786435.2013.790568

50. Mamedov TA, de Llano (2014) Are preformed Cooper pairs the cause for the pseudogap in superconductors? 94:4102–4114 https://doi.org/10.1080/14786435.2014.979903

51. Nambu Y (1960) Quasi-particles and gauge invariance in the theory of superconductivity. Phys Rev 117:648. https://doi.org/10.1103/PhysRev.117.648

52. Aguilera-Navarro VC, de Llano M, Solís MA (1999) Bose-Einstein condensation for general dispersion relations. Eur J Phys 20:177. https://doi.org/10.1088/0143-0807/20/3/307

53. de Llano M (2008) High-T_c superconductivity via BCS and BEC unification: a review. In: Martins BP (ed) Frontiers in superconductivity research. Nova, New York, pp 1–52

54. Adhikari SK, Casas M, Puente A et al (2000) Cooper pair dispersion relation for weak to strong coupling. Phys Rev B 62:8671. https://doi.org/10.1103/PhysRevB.62.8671

55. Casas M, Rigo A, de Llano M et al (1998) Bose-Einstein condensation with a BCS model interaction. Phys Lett A 245:55–61. https://doi.org/10.1016/S0375-9601(98)00377-6

56. Webb GW, Marsiglio F, Hirsch JE (2015) Superconductivity in the elements, alloys and simple compounds. Physica C 514:17–27. https://doi.org/10.1016/j.physc.2015.02.037

57. Chávez I, García LA, Grether M, de Llano M, Tolmachev VV (2019) Two-electron and two-hole cooper pairs in superconductivity. J Supercond Nov Magn 32:1633–1638. https://doi.org/10.1007/s10948-018-4890-6

58. Grether M, de Llano M, Baker GA Jr (2007) Bose-Einstein condensation in the relativistic ideal Bose gas. Phys Rev Lett 99:200406. https://doi.org/10.1103/PhysRevLett.99.200406

59. Andrenacci N, Perali A, Pieri P, Strinati GC (1999) Density-induced BCS to Bose-Einstein crossover. Phys Rev B 60:12410. https://doi.org/10.1103/PhysRevB.60.12410

60. Grether M, de Llano M, Ramírez S, Rojo O (2008) Intriguing role of hole-Cooper-pairs in superconductors and superfluids. Int J Mod Phys B 22:4367–4378. https://doi.org/10.1142/S0217979208050127

61. Ashcroft NW, Mermin ND (1976) Solid state physics. Saunders College Publishing, USA, pp. 38 and 48

62. Vakarchuk IO, Hryhorchak OI, Pastukhov VS, Prytula RO (2016) Effective mass of ^{4}He atom in superfluid and normal phases. Ukr J Phys 61(1):29. https://doi.org/10.15407/ujpe61.01.0029

63. Mao J, Wu DH, Peng JL et al (1995) Anisotropic surface impedance of $YBa_2Cu_3O_{7-\delta}$ single crystals. Phys Rev B 51:3316(R). https://doi.org/10.1103/PhysRevB.51.3316

64. Lemberger TR, Hetel I, Tsukada A et al (2011) Superconductor-to-metal quantum phase transition in overdoped $La_{2-x}Sr_xCuO_4$. Phys Rev B 83:140507(R). https://doi.org/10.1103/PhysRevB.83.140507

65. Shengelaya A, Aegerter CM, Romer S et al (1998) Muon-spin-rotation measurements of the penetration depth in the $YBa_2Cu_4O_8$ family of superconductors. Phys Rev B 58:3457. https://doi.org/10.1103/PhysRevB.58.3457

66. Regal CA, Jin DS (2003) Measurement of positive and negative scattering lengths in a fermi gas of atoms. Phys Rev Lett 90:230404. https://doi.org/10.1103/PhysRevLett.90.230404

67. Regal CA, Greiner M, Jin DS (2004) Observation of resonance condensation of fermionic atom pairs. Phys Rev Lett 92:040403. https://doi.org/10.1103/PhysRevLett.92.040403